

Journal Pre-proofs

Deeper insights into effect of activated carbon and nano-zero-valent iron addition on acidogenesis and whole anaerobic digestion

Ruming Wang, Chunxing Li, Nan Lv, Xiaofang Pan, Guanqing Cai, Jing Ning, Gefu Zhu

PII: S0960-8524(21)00009-2
DOI: <https://doi.org/10.1016/j.biortech.2021.124671>
Reference: BITE 124671

To appear in: *Bioresource Technology*

Received Date: 27 November 2020
Revised Date: 30 December 2020
Accepted Date: 1 January 2021

Please cite this article as: Wang, R., Li, C., Lv, N., Pan, X., Cai, G., Ning, J., Zhu, G., Deeper insights into effect of activated carbon and nano-zero-valent iron addition on acidogenesis and whole anaerobic digestion, *Bioresource Technology* (2021), doi: <https://doi.org/10.1016/j.biortech.2021.124671>

This is a PDF file of an article that has undergone enhancements after acceptance, such as the addition of a cover page and metadata, and formatting for readability, but it is not yet the definitive version of record. This version will undergo additional copyediting, typesetting and review before it is published in its final form, but we are providing this version to give early visibility of the article. Please note that, during the production process, errors may be discovered which could affect the content, and all legal disclaimers that apply to the journal pertain.

© 2021 Elsevier Ltd. All rights reserved.



1 **Deeper insights into effect of activated carbon and nano-zero-valent**

2 **iron addition on acidogenesis and whole anaerobic digestion**

3 **Ruming Wang^{a,b}, Chunxing Li^c, Nan Lv^{a,b}, Xiaofang Pan^a, Guanjing Cai^a, Jing Ning^a, Gefu**

4 **Zhu^{a,d*}**

5 *a Key Laboratory of Urban Pollutant Conversion, Institute of Urban Environment,*

6 *Chinese Academy of Sciences, Xiamen 361021, China*

7 *b University of Chinese Academy of Sciences, Beijing 100049, China*

8 *c Department of Environmental Engineering, Technical University of Denmark, DK-*

9 *2800 Lyngby, Denmark*

10 *d School of Environment and Nature Resources, Renmin University of China, Beijing*

11 *1000872, PR China*

12

* **Corresponding author**

E-mail: gfzhu@iue.ac.cn; Phone: 86-592-6190790; Fax: 86-592-6190790.

13 **Abstract:** Conductive materials presented promising advantages for enhancing
14 anaerobic digestion (AD) performance. This study evaluated the effects of activated
15 carbon (AC) and nano-zero-valent iron (nZVI) on the acidogenesis and whole AD to
16 explore their potential mechanisms. AC increased the content of lactic and propionic
17 acids in acidogenesis. nZVI increased the production of formic acid, acetic acid and
18 H₂ in acidogenesis, thus significantly promoted the methane yield in the whole AD.
19 Mechanism exploration proved that AC enriched *Trichococcus*, and
20 *norank_f__Bacteroidetes_vadinHA17*, and then improved the activity of enzymes
21 involved in the production of lactic and propionic acids. nZVI buffered the pH to
22 increase the activity of pyruvate formate-lyase (PFL) in formic acid production.
23 Furthermore, nZVI enriched the *Methanobacterium* which use H₂ and formic acid as
24 substrate. The research paves pathway for the efficient enhancement of conductive
25 materials added novel AD process.

26 **Key words:** Anaerobic digestion, Activated carbon, Nano-zero-valent iron,
27 Acidogenesis, Microbial community.

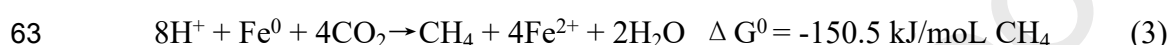
28 1. Introduction

29 Anaerobic digestion (AD) presented promising advantage in industrial and
30 agricultural waste treatment via converting organic waste into biogas in presence of
31 microorganism (Li et al., 2019). However, research showed that the process was still
32 limited by low acidification efficiency and the accumulation of volatile fatty acids
33 (VFAs) caused by slow syntrophic metabolism (Appels et al., 2011). Many studies
34 have shown that adding conductive materials to anaerobic digesters can accelerate and

35 stabilize the conversion of organic matter to methane (Dang et al., 2016; Zhang et al.,
36 2018). Previous research indicated that carbon-based materials including biochar,
37 activated carbon (AC) and carbon cloth or iron-based material including nano-zero-
38 valent iron (nZVI), magnetite and iron powder could promote the performance of AD
39 (Lim et al., 2020; Zhou et al., 2019; Li et al., 2019; Meng et al., 2013). Nevertheless,
40 the potential mechanism involving different conductive materials to improve the
41 performance of different stages of AD remains unclear.

42 Carbon materials are always used directly as an electron carrier to improve AD
43 efficiency by promoting electron transfer between syntrophic and methanogenic
44 partners (Liu et al., 2012a). Zhao et al. (2017) reported that after supplementing
45 granular activated carbon (GAC) in methanogenic phase, the methane production rate
46 improved by about 34%. Moreover, with a honeycomb pore structure, large specific
47 surface area and good adsorption performance, AC provides attachment sites for
48 microorganisms and helps reduce the impact of organic shock loads on the methane
49 production process (Aziz et al., 2011; Liu et al., 2012a). Also, it was reported that AC
50 could be used directly as an electron carrier to improve AD efficiency by promoting
51 electron transfer between syntrophic and methanogenic partners (Zhao et al., 2017;
52 Dang et al., 2016). nZVI, as a reducer, has high specific surface area, which is also
53 often used to enhance AD. Su et al. (2013) observed that adding 0.1% nZVI in
54 anaerobic system increased CH₄ production by 40.4%. As a reducing substance, it
55 could lower the ORP to provide a better anaerobic environment for methanogens (Liu
56 et al., 2011). On the other hand, nZVI can produce hydrogen through chemical

57 corrosion (Eq. (1)), which improves the efficiency of hydrogenotrophic
 58 methanogenesis (Hao et al., 2017). The produced Fe^{2+} from nZVI is an important
 59 element to many oxidoreductases, which can improve the metabolic activity of
 60 microorganisms.



64 Previous studies have compared the mechanisms between different types of
 65 conductive materials that enhance AD. However, the potential mechanisms of the
 66 conductive materials in each stage of AD are also different. In general, AD mainly
 67 involves four steps: hydrolysis, acidogenesis, acetogenesis, and methanogenesis.
 68 Firstly, the complex organic matter is hydrolyzed into simple organic matter by
 69 fermentation bacteria, and then these simple organics are converted into VFAs (lactic
 70 acid, acetic acid, formic acid, propionic acid, butyric acid and H_2/CO_2). VFAs can be
 71 converted into acetic and formic acids by acetogens, and finally they will be used by
 72 methanogens to produce methane in methanogenesis. However, there are few
 73 specifically produced substrates that can be used by methanogens, including H_2 (Eq.
 74 (4)), formic acid (Eq. (5)) and acetic acid (Eq. (6)). It can be seen that VFAs are
 75 important intermediates produced in the process of acidogenesis, acetogenesis and
 76 methanogenesis. Therefore, the concentration and composition of VFAs directly
 77 affects the efficiency of AD.





81 According to our knowledge, previous researches mainly focused on the
82 influence of conductive materials on the performance of AD, especially for the
83 methanogenesis. However, there has been less investigations into the potential
84 connection between the acidogenesis and the methanogenesis. [Xie et al. \(2020\)](#) found
85 that AC increased short-chain fatty acids production from algae during alkaline
86 anaerobic fermentation. Furthermore, it was reported that nZVI promoted VFAs
87 production, and acetic acid dominated in the batch system ([Jin et al., 2019](#)). AC
88 improves the activity of key hydrolase enzymes and the number of coding genes.
89 nZVI changes the community and metabolism of microorganisms by adjusting pH and
90 reducing ORP. However, there was no consensus on how conductive materials affect
91 the conversion of various products in the acidogenic phase. Additionally, the
92 relationship between microorganisms and materials are still unclear.

93 According to the above, AC and nZVI were selected as conductive materials to
94 deeply explore their effects on acidogenesis and whole AD in this study. One aim was
95 to explore the effects of different conductive materials on the conversion of metabolic
96 products during AD. Another objective was to dissect the microbial community
97 structure and metabolic mechanism in response to the addition of conductive
98 materials.

99 **2. Material and methods**

100 ***2.1 Substrates and inoculum***

101 The granular sludge used as seed sludge was collected from the starch
102 wastewater treatment plant in Xuzhou, China. The mixed liquor volatile suspended
103 solid (MLVSS) of inoculum was 23.33 g/L, and mixed liquor suspended solid
104 (MLSS) was 40.22 g/L.

105 In this experiment, artificial wastewater was used as the substrate. Glucose was
106 the carbon source and the chemical oxygen demand (COD) concentration was 2000
107 mg/L. In addition, NH_4Cl and KH_2PO_4 were used as nitrogen source and phosphorus
108 source, respectively. The ratio of COD: N: P in influent was 800: 5: 1. Trace metal
109 solution and mineral elements were added to the reaction system to ensure the growth
110 conditions of microorganisms. Their compositions were as follows: trace metal
111 solution (mg/L): $\text{FeCl}_2 \cdot 4\text{H}_2\text{O}$, 2; H_3BO_3 , 0.05; ZnCl_2 , 0.05; $\text{CuCl}_2 \cdot 2\text{H}_2\text{O}$, 0.038;
112 $\text{MnCl}_2 \cdot 4\text{H}_2\text{O}$, 0.05; $(\text{NH}_4)_6\text{Mo}_7\text{O}_{24} \cdot 4\text{H}_2\text{O}$, 0.05; AlCl_3 , 0.05; $\text{CoCl}_2 \cdot 6\text{H}_2\text{O}$, 0.05;
113 $\text{NiCl}_2 \cdot 6\text{H}_2\text{O}$, 0.09; $\text{Na}_2\text{WO}_4 \cdot 2\text{H}_2\text{O}$, 0.05; mineral elements (mg/L): CaCl_2 , 50;
114 $\text{MgCl}_2 \cdot 6\text{H}_2\text{O}$, 100; NaCl , 100.

115 **2.2 Batch Experimental design**

116 **2.2.1 Effect of conductive materials on acidogenesis**

117 To elucidate the effect of materials on the acidogenesis, 2-bromoethane sulfonate
118 (BES) was added with concentration of 30 mM at the beginning to inhibit the activity
119 of methanogens. The experiment was performed in 120 ± 4 mL serum bottle with 40
120 mL of substrate and 10 mL of inoculum. For AC group, 0.25 g AC (10-15 mm,
121 Sigma) was supplemented into the bottle. For nZVI group, 0.25 g nZVI (99.9% metals
122 basis, 100 nm, Sigma) was added into the bottle. The group without materials addition

123 was used as blank. For each group, the experiment was performed in triplicates. In
124 order to maintain strict anaerobic conditions, pure nitrogen (99.99%) was blown into
125 the reactor for 15 minutes, and then the bottles were sealed with rubber stoppers.
126 Finally, the reaction bottles were placed in a water bath shaker at 37°C and stirred at
127 160 rpm for 54 h. For chemical analysis, pH, VFAs and biogas components were
128 measured at 6, 9, 12, 15, 18, 30 and 54 h.

129 ***2.2.2 Effects of conductive materials on whole AD***

130 For the whole AD process, the experimental operation was consistent with the
131 acidogenesis but without adding 30 mM 2-BES to the bottles. All of these
132 experiments were conducted in triplicate. The bottles were incubated in a shaker at
133 37°C and stirred at 160 rpm for 31 days, and the biogas composition was monitored
134 every day.

135 ***2.3 Analytical methods***

136 Gas composition were analyzed by gas chromatography (FULI, GC9790II,
137 China) equipped with a TDX-01 (2 m long and 3 mm in inner diameter) as a
138 separation column and argon as a carrier gas. The GC parameters were set as follows:
139 column temperature, 120°C; detector temperature, 160°C; injection temperature,
140 160°C.

141 For the measurement of VFAs, the mixed solution was first centrifuged at 8000
142 rpm for 5 min, then filtered through a 0.22 µm filter, and the supernatant was acidified
143 with 2 M HCl to a pH below 2.0, and then stored at 4°C. Finally, ion chromatography
144 (ICS-3000, Dionex, USA) equipped with anion exchange column (Dionex IonPac™

145 AS11) including analytical column (Dionex IonPac™ AS11-HC, 4 mm×250 mm)
146 and protect column (Dionex IonPac™ AG11-HC, 4 mm×50 mm) were used for
147 VFAs measurement. The MLSS, MLVSS, COD, pH and ORP values were
148 determined according to Standard Methods ([APHA, 2012](#)).

149 The cumulative volume of CH₄ was calculated by multiplying the headspace
150 volume (74 mL) by the percentage of CH₄ (mL CH₄/mL) in the headspace as
151 determined by GC analysis. The gas sample taken from the batch reactor should take
152 into account the pressure in the batch reactor, which should equilibrate in the batch
153 reactor. Additionally, the obtained cumulative CH₄ production value was normalized
154 according to the ideal gas law ($PV = nRT$) in Standard Temperature and Pressure
155 (STP) conditions (0°C and 1 atm). The methane yield was expressed in NmLCH₄/g
156 COD ([Pan et al., 2019](#)).

157 The scanning electron microscope and X-ray energy dispersive spectroscopy
158 (SEM–EDS, S-4800, Japan) were used to determine morphology and chemical
159 composition of the sludge after acidogenesis. At the end of acidogenic phase, 5 mL
160 sludge sample was taken and centrifuged at 3000 rpm for 3 min, and then discard the
161 liquid supernatant and fixed in 2.5% glutaraldehyde for 4 h at 4°C. Then the samples
162 were washed twice times with 0.1 M phosphate buffer (pH=7.4), 10 minutes for each
163 step. After that, samples were dehydrated through a graded ethanol series, by 50%,
164 70%, 80% and 90%, 10 minutes for each step and keep samples at 4°C. Then, it was
165 dehydrated twice with 100% ethanol for 15 minutes each time. Finally, samples were
166 dried by critical point drying method for 24 h.

167 **2.4 Microbial community analysis**

168 Sludge samples were collected from the original inoculum, 9 h and 54 h of the
169 acidogenesis. In addition, the sludge samples were taken for microbiological analysis
170 at the end of whole AD. All samples were refrigerated at -20°C for subsequent
171 microbial analysis. DNA was extracted using Fast DNA Spin Kit for Soli (MP, USA)
172 method. The DNA concentration was determined by Nanodrop2000 (Thermo
173 Scientific, USA), and the purity was determined by measuring the absorbance ratio at
174 260/280 nm. The extracted DNA was stored at -20°C before measurement. The
175 microbial communities of the sludge were analyzed by high-throughput sequencing
176 on an Illumina MiSeq platform, which was performed by Majorbio Bio-Pharm
177 Technology Co. Ltd (Shanghai, China). The primers used for PCR amplification of
178 bacteria and archaea were 515Fmodf (GTGYCAGCMGCCGCGGTAA) and
179 806RmodR (GGACTACNVGGGTWTCTAAT), respectively, for the V4 region of
180 16S rRNA gene in each sludge sample.

181 Prediction of the metabolic function of bacteria and archaea in AD through
182 PICRUSt (Phylogenetic Investigation of Communities by Reconstruction of
183 Unobserved States) was based on the Galaxy platform against the KEGG (Kyoto
184 Encyclopedia of Gene and Genome) Orthology database ([Langille et al., 2013](#)).
185 Specific steps are as follows: 1) The gene function spectrum of their common ancestor
186 was inferred based on the full-length 16S rRNA sequence of the tested bacterial
187 genome; 2) The gene function spectrum of other untested species in the Greengenes
188 database was inferred, and the gene function prediction spectrum of the entire lineage

189 of archaea and bacteria was constructed; 3) The sequenced 16S rRNA gene sequence
190 data was compared with the Greengenes database to found the “reference sequence
191 nearest neighbor” of each sequencing sequence, and was classified as a reference
192 OTU; 4) The obtained OTU abundance matrix was corrected according to the rRNA
193 gene copy number of the “reference sequence nearest neighbor”; 5) The KEGG
194 Orthology (KO) information corresponding to the OTU was obtained through the
195 greengene id corresponding to each OTU; 6) According to the information in the
196 KEGG database, KO information can be obtained, and the abundance of each
197 functional category can be calculated according to the OTU abundance.

198 **2.5 Calculation**

199 Acidification efficiency (AE, %) was evaluated by the following Eq. (1):

$$200 \quad AE = \frac{COD_{VFAs}}{COD_{Influent}} \times 100\% \quad (1)$$

201 Where $COD_{Influent}$ is the concentration of influent COD (mg/L), COD_{VFAs} is the
202 concentration of effluent VFAs (mgCOD/L) (Lu et al., 2012).

203 **2.6 Statistical analysis**

204 Statistical analysis was conducted using EXCEL 2016 and SPSS 26 software. In
205 addition, Origin 8.0 was used for graphics drawing. Free online platform
206 (<http://www.i-sanger.com/>) was Majorbio I-Sanger Cloud platform. The operational
207 taxonomic unit (OTU) table was normalized, and the functional genes in AD were
208 analyzed by the KEGG Orthology (KO) (<http://www.kegg.jp/kegg/ko.html>). A p
209 value of <0.05 indicates statistical significance.

210 **3. Results and Discussion**

211 *3.1 Effect of conductive materials on VFAs, pH and gas content in acidogenesis*

212 The composition of VFAs and biogas content in each group were measured (Fig.
213 1). As shown in Fig. 1a-b, the main products were VFAs (including lactic acid, formic
214 acid, acetic acid and propionic acid), and H₂/CO₂ after blocking the methanogenesis.
215 In the initial 9 h, the pH of blank, AC and nZVI groups dropped sharply from 8.2, 8.1
216 and 8.1 to 6.2, 6.0 and 6.7 (Fig. 1c), respectively. It indicated that glucose was quickly
217 converted into acidic products after experiments. The lactic and formic acids both
218 accumulated in the three groups, while acetic and propionic acids showed small
219 generation. Lactic acid increased by 22.05% in AC group, but there has been little
220 change in nZVI added group. The formic acid in the three groups reached the
221 maximum value at 9 h with 169.57 mg/L, 192.95 mg/L and 193.99 mg/L,
222 respectively. Formic acid increased by 13.79% and 14.40%, in AC and nZVI added
223 systems, separately. This result indicated that AC mainly promoted the production of
224 lactic acid, while nZVI mainly promoted the formic acid generation in the early stage.
225 After 9 h, acetic acid and propionic acid gradually accumulated in the reactors. The
226 acetic acid content of the blank, AC and nZVI groups at 54 h were 513.60 mg/L,
227 531.55 mg/L and 613.50 mg/L, respectively. Acetic acid increased by 19.45% in
228 nZVI added systems, which was consistent with the previous research (Liu et al.,
229 2012b). Interestingly, the lactic acid and formic acid were completely consumed at the
230 end of reaction.

231 Lactic acid was the initial product of anaerobic fermentation. In the metabolism
232 of mixed bacteria, lactic acid was first produced through catalytic reduction of

233 pyruvate with lactate dehydrogenase. Afterwards, lactic acid was reduced to propionic
234 acid by propionate dehydrogenase (Lee et al., 2008). At 54 h, the contents of
235 propionic acid in the blank, AC and nZVI groups were 317.99 mg/L, 343.93 mg/L
236 and 310.28 mg/L, respectively. Due to promotion in lactic acid generation by AC, it's
237 the propionic acid reached the highest concentration at the end of the reaction. On the
238 other hands, ORP also affects fermentation products. The ORP of the blank, AC and
239 nZVI groups at the end of the reaction were -310 mV, -264 mV, and -335 mV,
240 respectively. Wang et al. (2006) reported that propionic acid was the main product at
241 ORP of -280 mV. As AC improved the ORP of the system, the production of
242 propionic acid was also increased. It was noteworthy that the proportion of propionic
243 acid dropped from 37.02% to 32.93% after adding nZVI. Since the fermentation
244 products in the anaerobic system were affected by ORP, the addition of nZVI to
245 reduce ORP may promote the conversion of propionic acid. Meng et al. (2013)
246 reported that the reduced ORP after adding ZVI can effectively increase the activity of
247 dehydrogenase, so the conversion rate of propionic acid increases from 43-77% to 67-
248 89%.

249 Formic and acetic acids are substrates that can be utilized by methanogens, and
250 formic acid is more easily used by methanogens than acetic acid in granular sludge
251 (Pan et al., 2016). The results showed that formic acid mainly accumulated in the
252 initial 9 h, while acetic acid was the dominant product at the end of the reaction. This
253 may be due to formic acid is not stable and is easily cracked into H_2 and CO_2 by
254 formate dehydrogenase (FDH) enzymes (Crable et al., 2011). Then H_2/CO_2 can be

255 converted into acetic acid as a substrate for homoacetogenic bacteria. As shown in
256 [Fig. 1b](#), the H₂ content in nZVI group was higher than that of AC and blank groups.
257 After adding nZVI, a large amount of H₂ was generated in the system. At 54 h, CO₂ in
258 the nZVI group was converted into acetic acid by reacting with H₂, and only little CO₂
259 was remained in nZVI group. Therefore, the content of acetic acid in the nZVI group
260 was the highest at the end of the reaction. Obviously, it suggested that adding nZVI
261 significantly promoted the generation of VFAs. This was consistent with the previous
262 research results, which obtained the maximum VFAs content after adding 30 mM
263 nZVI ([Zhou et al., 2020](#)). At the end of reaction, the acidification rates in the blank,
264 AC and nZVI groups were 53.64%, 56.21% and 57.77%, respectively. Hence, adding
265 nZVI in AD could promoted the conversion of more organic matter into VFAs and
266 increase the substrates (H₂, formic acid and acetic acid) for methanogens.

267 [Fig. 1](#)

268 ***3.2 Effects of conductive materials on methane production in whole AD***

269 Methane yield is an important indicator in reflecting the efficiency of AD. As
270 shown in [Fig. 2](#), the methane yield in AC added group was 241.18 mL CH₄/g COD,
271 which was lower than that of blank group of 250.11 mL CH₄/g COD. This result was
272 different from the previous research that adding GAC could promote methane yield in
273 methanogenesis by stimulating direct interspecies electron transfer (DIET) ([Zhao et](#)
274 [al., 2017](#)). This probably resulted from that AC mainly promoted the production of
275 lactic and propionic acids in the acidogenic phase, while DIET was not formed to
276 accelerate the syntrophic conversion of propionic acid to methane in this study.

277 Interestingly, the cumulative methane yield in nZVI added group was 309.89 mL
278 CH₄/g COD, which was significantly higher than that of the blank group. The
279 methane yield of nZVI added group increased by 23.9%, suggesting nZVI addition
280 could promote methane production. This could be mainly resulted from the following
281 three aspects. Firstly, nZVI created an environment conducive to the growth of
282 methanogens (Zhou et al., 2019). After the reaction, the pH value in nZVI group
283 (8.48) was higher than that of the AC group (6.87) and the blank group (6.88) (Table
284 1). The ORP value in nZVI group was -345 mV which was much lower than that of
285 AC (-197 mV) and blank group (-206 mV) (Table 1). Previous research also reported
286 that nZVI addition could lower the ORP value, providing a reductive condition (< -
287 200 mV) for methanogens (Liu et al., 2011). Secondly, Fe²⁺ released by the corrosion
288 of nZVI under anaerobic conditions (Eq. (1)) was an important element of various
289 redox enzymes. Hence, adding nZVI could improve the metabolic activity of
290 microorganisms (Wang et al., 2016). Thirdly, adding nZVI increased the available
291 substrates for methanogens (Feng et al., 2014). More formic acid was produced in
292 acidogenic phase, which could be used as a substrate for H₂-utilizing methanogens. In
293 addition, the H₂ produced by nZVI corrosion of in the early stage could further
294 convert CO₂ into CH₄ (Eqs. (1), (2)). However, due to the high Gibbs free energy of
295 the process of releasing H₂ through the corrosion of nZVI (Daniels et al., 1987), it was
296 necessary for H₂-consuming microorganisms to continuously consume hydrogen to
297 pull the corrosion of nZVI and keep the hydrogen partial pressure at a low level.
298 Additionally, iron can be used as an extracellular electron donor to participate in the

299 electron transfer of microbial metabolism (Newman & Kolter., 2000). nZVI also can
300 be used as a direct electron donor for methanogens (Eq. (3)) to accelerate the
301 corrosion of nZVI for methane enhancement (Karri et al., 2005).

302 **Fig. 2**

303 **Table 1**

304 **3.3 Microbial community analysis**

305 **3.3.1 Effects of conductive materials on microbial community in acidogenesis**

306 The microbial community in acidogenesis process was investigated and shown in
307 Fig 3a-b. In phylum level (Fig. 3a), *Firmicutes*, *Bacteroidetes* and *Chloroflexi*
308 dominated in conductive materials added conditions. These three phyla were also
309 reported to be common hydrolysis fermentation bacteria in solid waste, wastewater
310 and sludge treated by AD (Zhang et al., 2018). In addition, they can convert organic
311 matter into VFAs, following acetic acid and H₂/CO₂ generation. *Firmicutes* can
312 greatly promote the degradation of organic matter by proteases, cellulases and other
313 extracellular enzymes (Chen et al., 2017). *Bacteroidetes* is also a common hydrolysis
314 and fermentative bacteria in anaerobic systems, which can convert organic matter into
315 short-chain fatty acids (Chouari et al., 2005). Moreover, the bacteria in *Chloroflexi*
316 can degrade complex organic compounds (Roest et al., 2005). At 9 h, the total
317 abundance of the three bacterial phyla in the blank, AC and nZVI groups increased
318 from the original 60.26% to 77.94%, 83.72% and 81.52%, respectively, which were
319 consistent with the fermentation products. Correspondingly, AC added group obtained
320 the highest VFAs concentration, followed by nZVI and blank group. At 54 h, the

321 relative abundance of *Firmicutes* significantly increased in AC and nZVI groups with
322 44.35% and 43.70%, respectively. However, the *Bacteroidetes* decreased sharply in
323 the nZVI group (13.63%), and lower than the AC group (26.45%) and the blank group
324 (27.56%). The *Chloroflexi* decreased sharply in the AC group (10.85%) compared to
325 the blank (21.21%), while it was barely influenced by nZVI addition (20.68%).

326 The bacterial community is closely connected with the metabolites formation
327 (VFAs), which can further affect the methanogenesis process. At genus level (Fig.
328 3b), the dominant bacteria in the three groups were *Trichococcus* (phylum
329 *Firmicutes*), *norank_f__Bacteroidetes_vadinHA17* (phylum *Bacteroidetes*) and
330 *norank_f__Anaerolineaceae* (phylum *Chloroflexi*). *Trichococcus* is common acid-
331 producing bacteria, which mainly use glucose to produce lactic acid, formic acid,
332 acetic acid, and CO₂ (Wang et al., 2018b). *norank_f__Bacteroidetes_vadinHA17* is
333 reported to degrade glucose into acetic acid, propionic acid and H₂/CO₂ (Tan et al.,
334 2010; Ueki., 2006). Moreover, *norank_f__Anaerolineaceae* can convert propionic
335 acid into acetic acid (Vrieze et al., 2015). At 9 h, *Trichococcus* increased significantly
336 compared with initial condition, which maybe resulted in the increase of lactic and
337 formic acids (Fig. 1a). Furthermore, it was obvious that AC and nZVI addition
338 enriched *Trichococcus* compared to the blank group, leading to the higher
339 concentrations of lactic and formic acids. As a material with strong adsorption, high
340 porosity and high surface area, AC is conducive to the adhesion of microorganisms
341 (Aziz et al., 2011). Whereas, the enrichment of *Trichococcus* in nZVI-added system
342 may be due to the buffered pH. Wang et al. (2018b) reported that *Trichococcus* was

343 common among neutral pH bacteria. In three groups, compared to 9 h, the relative
344 abundance of *Trichococcus* and *norank_f__Bacteroidetes_vadinHA17* decreased at 54
345 h due to the consumption of substrates. However, the relative abundance of
346 *norank_f__Anaerolineacea* increased due to the production of propionic acid during
347 the reaction. The variation of VFAs was closely related to the microbial community.
348 At 54 h, it was showed that the content of lactic and formic acids decreased, while the
349 content of propionic and acetic acids increased significantly. Remarkably, nZVI
350 addition reduced the abundance of *norank_f__Bacteroidetes_vadinHA17*, while
351 enriched *norank_f__Anaerolineacea*, which indicated that nZVI may promote the
352 conversion of propionic acid. nZVI rapidly reduced the ORP, and the released Fe^{2+}
353 could promote sludge flocculation to form particles. Moreover, most of the
354 *norank_f__Anaerolineacea* are strictly anaerobic multicellular filamentous
355 microorganism. The flocculation of sludge can avoid destroying the structure of
356 bacterial filaments during the stirring process, which is more conducive to the growth
357 of *norank_f__Anaerolineacea* (Zhou et al., 2020). Therefore, at the end of the
358 acidogenesis, the acetic acid content in the nZVI group was the highest and the
359 propionic acid content was the least. Furthermore, it was worth noting that
360 *Clostridium* (phylum *Firmicutes*), increased from 0.34%, 0.43% and 0.13% at 9h to
361 1.45%, 2.05% and 0.42% at 54h in blank, AC and nZVI, respectively. As the most
362 common homoacetogen (Drake et al., 2006), the growth of *Clostridium* indicated that
363 H_2 and CO_2 were used as substrates by through homoacetogenesis to generate acetic
364 acid in the late stage of the reaction.

365

Fig. 3

366 **3.3.2 Effects of conductive materials on the microbial community in whole AD**

367 The relative abundances of methanogens at phylum and genus levels in each
368 group were shown in Fig. 3c-d. At phylum level (Fig. 3c), *Euryarchaeota* was the
369 main phyla in the blank, AC and nZVI groups (counting for 97.96%, 98.58% and
370 99.19%, respectively). At the genus level (Fig. 3d), *Methanosaeta* and
371 *Methanobacterium* dominated in three groups. *Methanosaeta*, the well-known acetate-
372 utilizing methanogens, accounted for 56.02% in nZVI group which was lower than
373 that in AC group (58.52%) and blank group (64.03%). As typical hydrogen-utilizing
374 methanogens, the abundances of *Methanobacterium* were 19.83%, 30.44% and
375 39.44% in the blank, AC and nZVI groups, respectively. Compared with blank, the
376 increase of relative abundance of *Methanobacterium* in AC group was resulted from
377 the enrichment of acid-producing bacteria to produce more H₂ in the early stage after
378 AC addition. Chen et al. (2014) reported that GAC could accelerate the syntrophic
379 conversion of VFAs to methane via DIET in defined co-cultures of *G.*
380 *metallireducens* and *Methanosarcina barkeri* as well as in some mixed cultures (Zhao
381 et al., 2015). However, the abundances of *Methanosaeta* and *Methanosarcina* in the
382 AC group decreased compared to the blank group, while the abundance of
383 *Methanobacterium* increased significantly. Thus, DIET was not formed to promote
384 methane production in this study. Therefore, AC did not show a promoting effect in
385 the whole AD process. Particularly, the significant increase of *Methanobacterium* in
386 the nZVI group may be due to the generation of hydrogen from nZVI addition (Fig.

387 2). Moreover, nZVI promoted the production of formic acid and the increase of H₂
388 content during acidogenic phase (Fig. 1), which supplied substrate for
389 *Methanobacterium*. Similarly, more methane generation in the nZVI group maybe
390 resulted from the higher abundance of *Methanobacterium*. In the nZVI group, the
391 content of H₂ and formic acid significantly increased in the early stage, while the
392 accumulation of acetic acid occurred in the later stage of the acidogenesis. However,
393 H₂ and formic acid were thermodynamically easier to be used by methanogens than
394 acetic acid (Eqs. (4)-(6)). Therefore, the increase in H₂ and formic acid content in the
395 early stage provided a suitable substrate for hydrogenotrophic methanogens.

396 **3.4 Characteristics of conductive materials and mechanism analysis on AD**

397 **3.4.1 Impacts of conductive materials on sludge characteristics**

398 SEM observation showed that the interior and surface of the sludge in the three
399 groups were dominated by bacillus and cocci. The microorganisms in the blank group
400 were scattered on the surface of the sludge. Interestingly, a pore structure was formed
401 after the addition of AC, so bacillus and cocci were adsorbed on the inside and surface
402 of the sludge. Remarkably, the microorganisms in the nZVI group were tightly
403 connected and wrapped. Zhang et al. (2011) reported that the cocci-shaped on the
404 surface of sludge in ZVI packed reactor was related to the acidogens. Due to the
405 electrostatic interaction and high specific surface area, nZVI was adsorbed on the cell
406 surface. Therefore, the elemental iron on the cell surface increased significantly after
407 nZVI addition. The released Fe²⁺ might penetrate into the microbial cells and
408 participate in the synthesis of key enzymes.

409 3.4.2 The relationship between bacteria and environmental variables

410 Redundancy analysis (RDA) was carried out to explore the correlation between 6
411 environmental factors and the 3 main bacterial communities (*Trichococcus*,
412 *norank_f__Bacteroidetes_vadinHA17* and *norank_f__Anaerolineaceae*) in the
413 acidogenesis process. As shown in Fig. 4, the distribution of the samples changed
414 significantly, and the 7 samples were well separated in groups. The original sample
415 was separated from the blank, AC and nZVI groups. The results showed that great
416 difference occurred between different groups. Obviously, lactic acid and formic acid
417 were clustered closely, and acetic acid and propionic acid were also positively
418 correlated. This confirmed the accumulation of lactic acid and formic acid in the early
419 stage of acidogenesis, while the accumulation of acetic acid and propionic acid in the
420 later stage. In addition, pH and VFAs (lactic acid, formic acid) showed a strong
421 negative correlation, indicating that the accumulation of lactic acid and formic acid in
422 the early stage of acidogenesis rapidly reduced the pH. Lactic acid showed a strong
423 positive correlation in the AC group (Fig. 4), indicating that AC had a significant
424 promoting effect on lactic acid. Remarkably, the two groups with nZVI added were
425 positively correlated with VFAs. These proved that conductive materials play a
426 leading role in promoting the hydrolysis and acidogenesis of organics. In addition,
427 RDA results can also reveal the distribution of microbial communities. *Trichococcus*
428 was positively correlated with formic acid, acetic acid and H₂. At 9 h, compared with
429 the original sludge, the abundance of *Trichococcus* in the three systems all increased
430 significantly, so the content of fermentation products also increased accordingly. As

431 expected, *norank_f__Anaerolineaceae* showed a positive correlation with acetic acid.
432 Conversely, *norank_f__Bacteroidetes_vadinHA17* did not have a positive correlation
433 with propionic acid. It was speculated that the conversion of VFAs was not only
434 related to the abundance of microorganisms, but also related to the metabolic activity
435 of microorganisms. In addition, AC was located near the *Trichococcus* and
436 *norank_f__Bacteroidetes_vadinHA17*, indicating that AC had a positive effect on
437 their growth. Furthermore, *Trichococcus* and *norank_f__Anaerolineaceae* were
438 distributed closely to nZVI, indicating that adding nZVI was beneficial to their
439 growth. The RDA analysis showed that the bacterial communities were affected by
440 AC and nZVI which explains the different performance in the AC and nZVI groups.

441 Fig. 4

442 3.4.3 Mechanism analysis of conductive materials on AD

443 In the acidogenesis period, AC promoted the production of lactic and propionic
444 acids, while nZVI promoted the production of formic and acetic acids. In order to
445 reveal the promotion mechanism of AC and nZVI, based on the function prediction
446 analysis, the related functional enzyme-encoding gene in the blank, AC and nZVI
447 groups were analyzed. As shown in Fig. 5, the addition of materials enhanced the
448 activity of key enzymes compared to the blank group. The abundance of encoding
449 genes of lactate dehydrogenase, propionate CoA-transferase, butyryl-CoA
450 dehydrogenase and propionyl-CoA synthetase related to lactic and propionic acids
451 increased in the AC group, indicating that AC promoted the production of lactic and
452 propionic acids. Due to the adsorption and porous structure of AC, acid-producing

453 bacteria were enriched in the anaerobic system. Hence, the lactic acid content in the
454 AC group was the highest (Fig. 1a). Subsequently, as an intermediate product in the
455 process of reducing pyruvic acid to propionic acid, lactic acid was consumed by
456 producing propionic acid. The conversion from pyruvate to lactic and propionic acids
457 requires the consumption of NADH. It was reported that ORP can influent
458 intracellular NADH/NAD⁺ ratio, which in turn affect enzyme activity and metabolites
459 (Liu et al., 2013). Tian et al. (2015) reported that when ORP was -250 mV, the highest
460 NADH appeared in the system. At the end of the reaction, the ORP value in the AC
461 group was -264 mV, so AC appropriately increased the ORP value of the system and
462 promoted the production of NADH. Therefore, the activity of the enzyme was
463 enhanced.

464 In addition, the products of concern were formic acid, acetic acid and H₂/CO₂,
465 which were substrates available for methanogens. In the absence of oxygen, pyruvate
466 can be catalyzed by pyruvate-ferredoxin oxidoreductase (POR) to acetyl-CoA and
467 CO₂, or by pyruvate formate-lyase (PFL) to formate and acetyl-CoA (Knappe et al.,
468 1974). In the initial 9 h, formic acid in the three groups accumulated to the maximum
469 value. At this time, the prediction of functional enzyme-encoding genes showed that
470 the abundance of PFL-encoding genes in the three groups increased significantly
471 compared to original sludge. The blank, AC and nZVI groups increased by 0.49-fold,
472 1.74-fold, and 1.94-fold, respectively. Due to nZVI decreased ORP, it provided a
473 favorable environment for the growth of acid-producing bacteria (Luo et al.,2014). On
474 the other hand, mainly enzymes contain iron-sulfur reducing clusters, the Fe²⁺

475 released after the addition of nZVI could greatly increase the activity of the enzyme
476 (Yang & Wang, 2018). Also, it was reported that the optimum pH for PFL was 7.0
477 (Pecher et al., 1982). Therefore, nZVI buffered the pH of the system and provided a
478 more suitable condition for the expression of PFL. Consistently, the formic acid
479 production in the nZVI group was the highest (Fig. 1a). Whereas, when
480 methanogenesis was inhibited, formic acid can be cleaved into H₂/CO₂ by formate
481 dehydrogenase, and H₂/CO₂ can be converted into acetic acid via the Wood-
482 Ljungdahl pathway. At 54 h, the abundance of genes encoding formate dehydrogenase
483 and methyletransferase increased slightly compared to 9 h, while other enzyme-
484 encoding genes have declined. Therefore, the results showed that in batch systems,
485 formic acid was mainly produced in the early stage, and acetic acid was generated in
486 the later stage of acidogenesis. The addition of nZVI could release more H₂, and the
487 increase of H₂ accelerated the consumption of CO₂ and promoted the homoacetogenic
488 process. Therefore, at the end of the reaction, CO₂ was completely consumed in the
489 nZVI group, and the acetic acid was higher than that of the other two groups.

490 From the perspective of the methanogenesis process, nZVI had a significant
491 promoting effect on the production of methane. The substrates produced in the
492 acidogenic phase that can be utilized by methanogens were mainly acetic acid, formic
493 acid and H₂/CO₂, which are mainly involved two methanogenic pathways, including
494 acetoclastic and hydrogenotrophic pathways. Obviously, 5-methyl-THMPT is a
495 common intermediate for two methanogenesis pathways, catalyzed by acetyl-CoA
496 decarbonylase during acetate-dependent methanogenesis and 5,10-

497 methylenetetrahydromethanopterin reductase during CO₂-dependent methanogenesis
498 (Wang et al., 2018a). In the process of acetoclastic methanogenesis, acetic acid is
499 finally converted into CH₄ and CO₂ by the action of various enzymes such as acetyl-
500 CoA decarbonylase, tetrahydromethanopterin S-methyltransferase and methyl-
501 coenzyme M reductase. In the hydrogenotrophic methanogenesis, H₂/CO₂ or formic
502 acid requires multiple steps to be converted into methane. CO₂ is gradually converted
503 into formyl, methylene and methyl groups under the action of various enzymes, and
504 then into methane (Guo et al., 2015). Moreover, the formic acid produced in the
505 acidogenic stage can also be used as a substrate for methanogens, but free formic acid
506 cannot be directly used by methanogens. Formic acid is first oxidized to CO₂ by FDH,
507 and accompanied by the production of F₄₂₀H₂, and then converted into methane
508 through the CO₂ reduction pathway (Crable et al., 2011). As shown in Fig. 5, after the
509 addition of nZVI, encoding gene of the FDH that catalyzed the conversion of formic
510 acid oxidation and CO₂ reduction had a higher abundance. Also, the abundances of
511 the encoding genes of functional enzymes for the hydrogenotrophic pathway was
512 richer than acetoclastic pathway. It indicated that nZVI promoted the production of
513 formic acid in the acidogenic phase, which could provide a rich substrate for
514 hydrogen-utilizing methanogens. The addition of nZVI greatly enhanced the
515 hydrogenotrophic pathway, and the hydrogen in the system may be produced by the
516 chemical corrosion of the nZVI or produced in acidogenesis process, which was
517 consistent with the results of Feng et al. (2014). Besides, nZVI can be used as a direct
518 electron donor to reduce CO₂ to methane.

519

Fig. 5

520 4. Conclusions

521 The present study systematically investigated the effect of AC and nZVI addition
522 on acidogenesis and whole anaerobic digestion process. AC enriched the
523 *Trichococcus* and *norank_f__Bacteroidetes_vadinHA17* by its pore structure,
524 indicating that AC promoted the production of lactic and propionic acids in
525 acidogenic phase. nZVI significantly improved the activity of functional enzymes by
526 buffering pH and releasing Fe^{2+} , thereby increased the production of formic acid in
527 acidogenic phase. In addition, nZVI enriched the hydrogenotrophic methanogens in
528 whole AD for higher CH_4 yield. Thus, adding nZVI is a promising strategy to increase
529 both acidogenesis and whole AD process for higher efficiency.

530 Acknowledgements

531 This work was supported by the National Natural Science Foundation of China
532 (grant numbers: 51678553, 21876167 and 52070176) and the National Key Research
533 and Development Program of China (grant number: 2017YFD0800804-03).

534 References

- 535 1. APHA, 2012. Standard Methods for the Examination of Water and Wastewater,
536 22th ed. American Public Health Association, Washington, DC, USA.
- 537 2. Appels, L., Lauwers, J., Degreve, J., Helsen, L., Lievens, B., Willems, K., Van
538 Impe, J.V., Dewil, R., 2011. Anaerobic digestion in global bio-energy production:
539 potential and research challenges. *Renew. Sust. Energ. Rev.* 15(9), 4295-4301.
- 540 3. Aziz, S.Q., Aziz, H.A., Yusoff, M.S., Bashir, M.J., 2011. Landfill leachate

- 541 treatment using powdered activated carbon augmented sequencing batch reactor
542 (SBR) process: optimization by response surface methodology. *J. Hazard. Mater.*
543 189(1-2), 404-413.
- 544 4. Chen, S.S., Rotaru, A.E., Liu, F.H., Philips, J., Woodard, T.L., Nevin, K.P.,
545 Lovley, D.R., 2014. Carbon cloth stimulates direct interspecies electron transfer
546 in syntrophic cocultures. *Bioresour. Technol.* 173, 82-86.
- 547 5. Chen, Y., Jiang, X., Xiao, K.K., Shen, N., Zeng, R.J., Zhou, Y., 2017. Enhanced
548 volatile fatty acids (VFAs) production in a thermophilic fermenter with stepwise
549 pH increase - Investigation on dissolved organic matter transformation and
550 microbial community shift. *Water Res.* 112, 261-268.
- 551 6. Chouari, R., Le Paslier, D., Daegelen, P., Ginestet, P., Weissenbach, J., Sghir, A.,
552 2005. Novel predominant archaeal and bacterial groups revealed by molecular
553 analysis of an anaerobic sludge digester. *Environ. Microbiol.* 7(8), 1104-1115.
- 554 7. Crable, B.R., Plugge, C.M., McInerney, M.J., Stams, A.J., 2011. Formate
555 formation and formate conversion in biological fuels production. *Enzyme Res.*
556 2011, 532536.
- 557 8. Dang, Y., Holmes, D.E., Zhao, Z.Q., Woodard, T.L., Zhang, Y.B., Sun, D.Z.,
558 Wang, L.Y., Nevin, K.P., Lovley, D.R., 2016. Enhancing anaerobic digestion of
559 complex organic waste with carbon-based conductive materials. *Bioresour.*
560 *Technol.* 220, 516-522.
- 561 9. Daniels, L., Belay, N., Rajagopal, B.S., Weimer, P.J., 1987. Bacterial
562 Methanogenesis and Growth from CO₂ with Elemental Iron as the Sole Source of

- 563 Electrons. Science 237(4814), 509-511.
- 564 10. Drake, H.L., Gößner, A.S., Daniel, S.L., 2008. Old acetogens, New light. Ann N
565 Y Acad Sci, 1125(1):100-128.
- 566 11. Feng, Y.H., Zhang, Y.B., Quan, X., Chen, S., 2014. Enhanced anaerobic digestion
567 of waste activated sludge digestion by the addition of zero valent iron. Water Res.
568 52, 242–250.
- 569 12. Guo, J.H., Peng, Y.Z., Ni, B.J., Han, X.Y., Fan, L., Yuan, Z.G., 2015. Dissecting
570 microbial community structure and methane-producing pathways of a full-scale
571 anaerobic reactor digesting activated sludge from wastewater treatment by
572 metagenomic sequencing. Microb. Cell Fact. 14, 33.
- 573 13. Hao, X.D., Wei, J., Loosdrecht, M.C.M.V., Cao, D.Q., 2017. Analysing the
574 mechanisms of sludge digestion enhanced by iron. Water Res. 117, 58-67.
- 575 14. Jin, Y., Gao, M., Li, H.G., Lin, Y.J., Wang, Q.H., Tu, M.B., Ma, H.Z., 2019.
576 Impact of nanoscale zerovalent iron on volatile fatty acid production from food
577 waste: key enzymes and microbial community. J. Chem. Technol. Biot. 94(10),
578 3201-3207.
- 579 15. Karri, S., Sierra-Alvarez, R., Field, J.A., 2005. Zero valent iron as an electron-
580 donor for methanogenesis and sulfate reduction in anaerobic sludge. Biotechnol.
581 Bioeng. 92(7), 810-819.
- 582 16. Knappe, J., Blaschkowski, H.P., Gröbner, P., Schmitt, T., 1974. Pyruvate
583 formate-lyase of *Escherichia coli*: the acetyl-enzyme intermediate. Eur. J.
584 Biochem. 50(1), 253-263.

- 585 17. Langille, M.G.I., Jesse, Z., J Gregory, C., Daniel, M.D., Dan, K., Reyes, J.A.,
586 Clemente, J.C., Burkepille, D.E., Thurber, R.L., Vega, Rob, K., 2013. Predictive
587 functional profiling of microbial communities using 16S rRNA marker gene
588 sequences. *Nat. Biotechnol.* 31, 814–821.
- 589 18. Lee, H.S., Salerno, M.B., Rittmann, B.E., 2008. Thermodynamic evaluation on
590 H₂ production in glucose fermentation. *Environ. Sci. Technol.* 42(7), 2401-2407.
- 591 19. Li, Y., Chen, Y.G., Wu, J., 2019. Enhancement of methane production in
592 anaerobic digestion process: A review. *Appl. Energy* 240, 120-137.
- 593 20. Lim, E.Y., Tian, H.L., Chen, Y.Y., Ni, K.W., Zhang, J.X., Tong, Y.W., 2020.
594 Methanogenic pathway and microbial succession during start-up and stabilization
595 of thermophilic food waste anaerobic digestion with biochar. *Bioresour. Technol.*
596 314, 123751.
- 597 21. Liu, C.G., Xue, C., Lin, Y.H., Bai, F.W., 2013. Redox potential control and
598 applications in microaerobic and anaerobic fermentations. *Biotechnology Adv.*
599 31(2), 257-265.
- 600 22. Liu, F.H., Rotaru, A.E., Shrestha, P.M., Malvankar, N.S., Nevin, K.P., Lovley,
601 D.R., 2012a. Promoting direct interspecies electron transfer with activated
602 carbon. *Energy Environ. Sci.* 5(10), 8982.
- 603 23. Liu, Y.W., Zhang, Y.B., Quan, X., Chen, S., Zhao, H.M., 2011. Applying an
604 electric field in a built-in zero valent iron-anaerobic reactor for enhancement of
605 sludge granulation. *Water Res.* 45(3), 1258-1266.
- 606 24. Liu, Y.W., Zhang, Y.B., Zhao, Z.Q., Li, Y., Quan, X., Chen, S., 2012b. Enhanced

- 607 azo dye wastewater treatment in a two-stage anaerobic system with Fe⁰ dosing.
608 Bioresour. Technol. 121, 148-153.
- 609 25. Lu, L., Xing, D.F., Liu, B.F., Ren, N.Q., 2012. Enhanced hydrogen production
610 from waste activated sludge by cascade utilization of organic matter in microbial
611 electrolysis cells. Water Res. 46 (4), 1015-1026.
- 612 26. Luo, J.Y., Feng, L.Y., Chen, Y.G., Li, X., Chen, H., Xiao, N.D., Wang, D.B.,
613 2014. Stimulating shortchain fatty acids production from waste activated sludge
614 by nano zero-valent iron. J. Biotechnol. 187, 98-105.
- 615 27. Meng, X.S., Zhang, Y.B., Li, Q., Quan, X. 2013., Adding Fe⁰ powder to enhance
616 the anaerobic conversion of propionate to acetate. Biochem. Eng. J. 73, 80-85.
- 617 28. Newman, D.K., Kolter, R., 2000. A role for excreted quinones in extracellular
618 electron transfer. Nature 405, 94-97.
- 619 29. Pan, X.F., Angelidaki, I., Alvarado-Morales, M., Liu, H.G., Liu, Y.H., Huang, X.,
620 Zhu, G.F., 2016. Methane production from formate, acetate and H₂/CO₂; focusing
621 on kinetics and microbial characterization. Bioresour. Technol. 218, 796-806.
- 622 30. Pan, X.F., Lv, N., Li, C.X., Ning, J., Wang, T., Wang, R.M., Zhou, M.D., Zhu,
623 G.F., 2019. Impact of nano zero valent iron on tetracycline degradation and
624 microbial community succession during anaerobic digestion. Chem. Eng. J. 359,
625 662-671.
- 626 31. Pecher, A., Blaschkowski, H.P., Knappe, K., Böck. A., 1982. Expression of
627 pyruvate formate-lyase of *Escherichia coli* from the cloned structural gene. Arch.
628 Microbiol. 132, 365-371.

- 629 32. Roest, K., Heilig, H.G.H.J., Smidt, H., Vos, W.M.D., Stams, A.J.M., Akkermans,
630 A.D.L., 2005. Community analysis of a full-scale anaerobic bioreactor treating
631 paper mill wastewater. *Syst. Appl. Microbiol.* 28(2), 175-185.
- 632 33. Su, L.H., Shi, X.L., Guo, G.Z., Zhao, A.H., Zhao, Y.C., 2013. Stabilization of
633 sewage sludge in the presence of nanoscale zero-valent iron (nZVI): abatement of
634 odor and improvement of biogas production. *J. Mater. Cycles Waste* 15, 461-468.
- 635 34. Tan, R., Miyanaga, K., Toyama, K., Uy, D., Tanji, Y., 2010. Changes in
636 composition and microbial communities in excess sludge after heat-alkaline
637 treatment and acclimation. *Biochem. Eng. J.* 52(2-3), 151-159.
- 638 35. Tian, X.W., Zhang, N., Yang, Y., Wang, Y.H., Chu, J., Zhuang, Y.P., Zhang,
639 S.L., 2015. The effect of redox environment on L-lactic acid production by
640 *Lactobacillus paracasei*-A proof by genetically encoded in vivo NADH
641 biosensor. *Process Biochem.* 50(12), 2029-2034.
- 642 36. Ueki, A., Akasaka, H., Suzuki, D., Ueki, K., 2006. *Paludibacter propionicigenes*
643 gen. nov., sp. nov., a novel strictly anaerobic, Gram-negative, propionate-
644 producing bacterium isolated from plant residue in irrigated rice-field soil in
645 Japan. *Int. J. Syst. Evol. Micr.* 56(1), 39-44.
- 646 37. Vrieze, J.D., Gildemyn, S., Vilchez-Vargas, R., Jáuregui, R., Pieper, D.H.,
647 Verstraete, W., Boon, N., 2015. Inoculum selection is crucial to ensure
648 operational stability in anaerobic digestion. *Appl. Environ. Microbiol.* 99:189-99.
- 649 38. Wang, L., Zhou, Q., Li, F.T. 2006. Avoiding propionic acid accumulation in the
650 anaerobic process for biohydrogen production. *Biomass Bioenergy* 30(2), 177-

- 651 182.
- 652 39. Wang, T., Zhang, D., Dai, L.L., Chen, Y.G., Dai, X.H., 2016. Effects of Metal
653 Nanoparticles on Methane Production from Waste-Activated Sludge and
654 Microorganism Community Shift in Anaerobic Granular Sludge. *Sci. Rep.* 6,
655 25857.
- 656 40. Wang, T., Zhang, D., Dai, L.L., Dong, B., Dai, X.H., 2018a. Magnetite
657 Triggering Enhanced Direct Interspecies Electron Transfer: A Scavenger for the
658 Blockage of Electron Transfer in Anaerobic Digestion of High-Solids Sewage
659 Sludge. *Environ Sci Technol*, 52(12), 7160-7169.
- 660 41. Wang, Z.Z., Yin, Q.D., Gu, M.Q., He, K., Wu, G.X., 2018b. Enhanced azo dye
661 reactive red 2 degradation in anaerobic reactors by dosing conductive material of
662 ferrous oxide. *J. Hazard. Mater.* 357, 226-234.
- 663 42. Xie, J., Chen, Y.Z., Duan, X., Feng, L.Y., Yan, Y.Y., Wang, F., Zhang, X.Z.,
664 Zhang, Z.G., Zhou, Q., 2019. Activated carbon promotes short-chain fatty acids
665 production from algae during anaerobic fermentation. *Sci. Total Environ.* 658,
666 1131-1138.
- 667 43. Yang, G., Wang, J., 2018. Various additives for improving dark fermentative
668 hydrogen production: A review. *Renew. Sust. Energ. Rev.* 95, 130-146.
- 669 44. Zhang, Y.B., An, X.L., Quan, X., 2011. Enhancement of sludge granulation in a
670 zero valence iron packed anaerobic reactor with a hydraulic circulation. *Process*
671 *Biochem.* 46(2), 568 471-476.
- 672 45. Zhang, Z.H., Gao, P., Cheng, J.Q., Liu, G.H., Zhang, X.Q., Feng, Y.J., 2018.

- 673 Enhancing anaerobic digestion and methane production of tetracycline
674 wastewater in EGSB reactor with GAC/NZVI mediator. *Water Res.* 136, 54-63.
- 675 46. Zhao, Z.Q, Li, Y., Quan, X., Zhang, Y.B., 2017. Towards engineering
676 application: Potential mechanism for enhancing anaerobic digestion of complex
677 organic waste with different types of conductive materials. *Water Res.* 115, 266-
678 277.
- 679 47. Zhao, Z.Q., Zhang, Y.B., Woodard, T.L., Nevin, K.P., Lovley, D.R., 2015.
680 Enhancing syntrophic metabolism in up-flow anaerobic sludge blanket reactors
681 with conductive carbon materials. *Bioresour. Technol.* 191, 140-145.
- 682 48. Zhou, J., You, X.G., Jia, T.T., Niu, B.W., Gong, L., Yang, X.Q., Zhou, Y., 2019.
683 Effect of nanoscale zero-valent iron on the change of sludge anaerobic digestion
684 process. *Environ. Technol.* 41(24), 3199-3209.
- 685 49. Zhou, J., You, X.G., Niu, B.W., Yang, X.Q., Gong, L., Zhou, Y., Wang, J.,
686 Zhang, H.N., 2020. Enhancement of methanogenic activity in anaerobic digestion
687 of high solids sludge by nano zero-valent iron. *Sci. Total Environ.* 703, 135532.

688 **Credit Author Statement**

689 **Ruming Wang:** Conceptualization, Methodology, Formal analysis, Investigation, Data
690 curation, Writing-original Draft. **Chunxing Li:** Resources, Formal analysis, Validation,
691 Writing-review & editing. **Nan Lv:** Supervision, Validation. **Xiaofang Pan:** Resources,
692 Funding acquisition, Supervision. **Guanjing Cai:** Reviewing and Editing. **Jing Ning:**
693 Supervision, Formal analysis. **Gefu Zhu:** Project administration, Funding acquisition,
694 Supervision.

695

696 50.

697 **Declaration of interests**

698

699 The authors declare that they have no known competing financial interests or personal
700 relationships that could have appeared to influence the work reported in this paper.

701

702 The authors declare the following financial interests/personal relationships which

703 may be considered as potential competing interests:

704

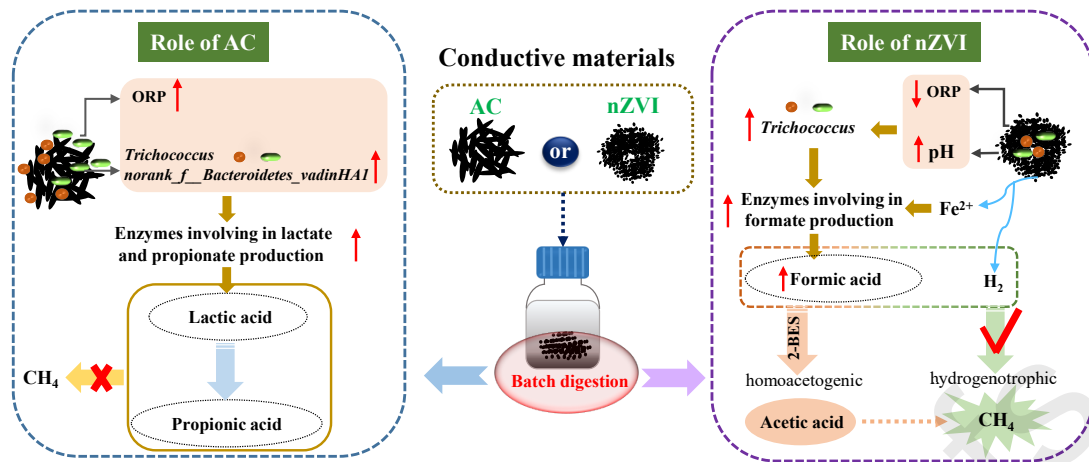
705

706

707

708

709 51.



710

711 52.

712 **Figure Captions**713 **Fig. 1** Variation in VFAs (a), gas content (b) and pH (c) during the acidogenesis.714 **Fig. 2** Methane yield in blank, AC and nZVI added groups.715 **Fig. 3** The distribution of bacterial communities at phylum level (a) and genus level

716 (b) in acidogenesis, and the comparison of archaea community structures of three

717 groups at phylum level (c) and genus level (d) in whole AD.

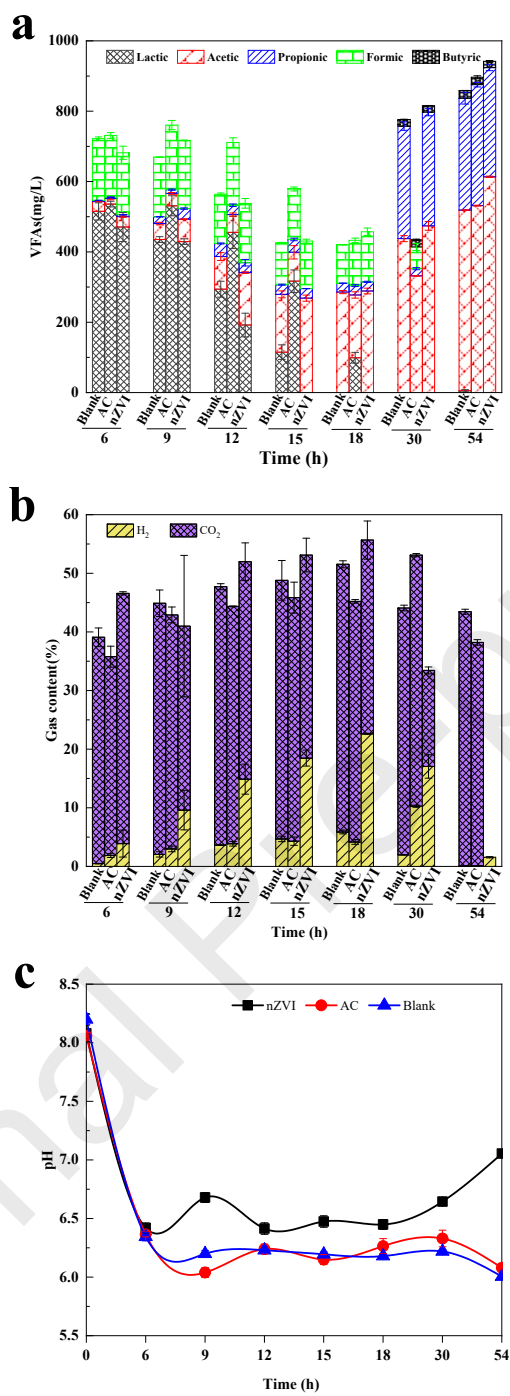
718 **Fig.4** The connection between different samples, bacterial communities and

719 environmental factors.

720 **Fig. 5** The abundance variations of relevant functional enzyme-encoding genes

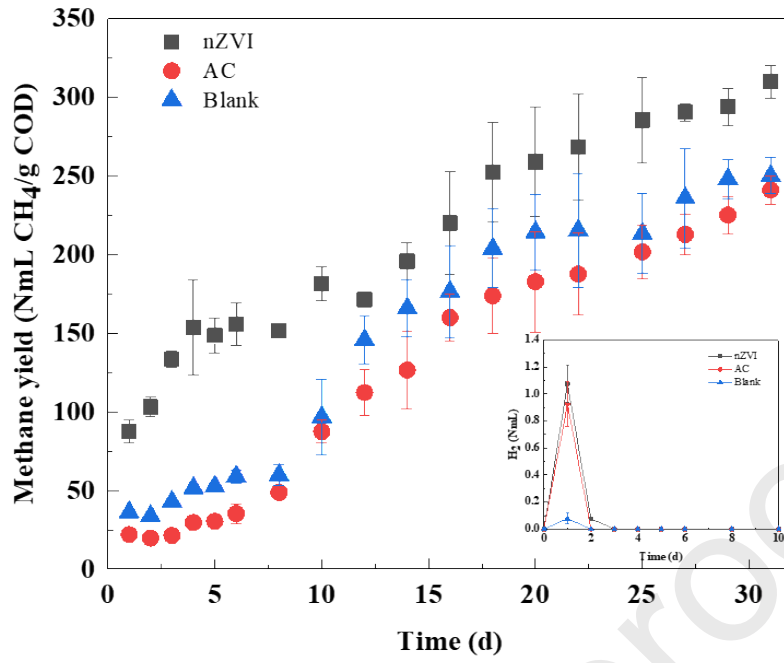
721 involved in the pyruvate metabolism between acidogens and methanogens at three

722 groups.



724

Fig. 1



725

726

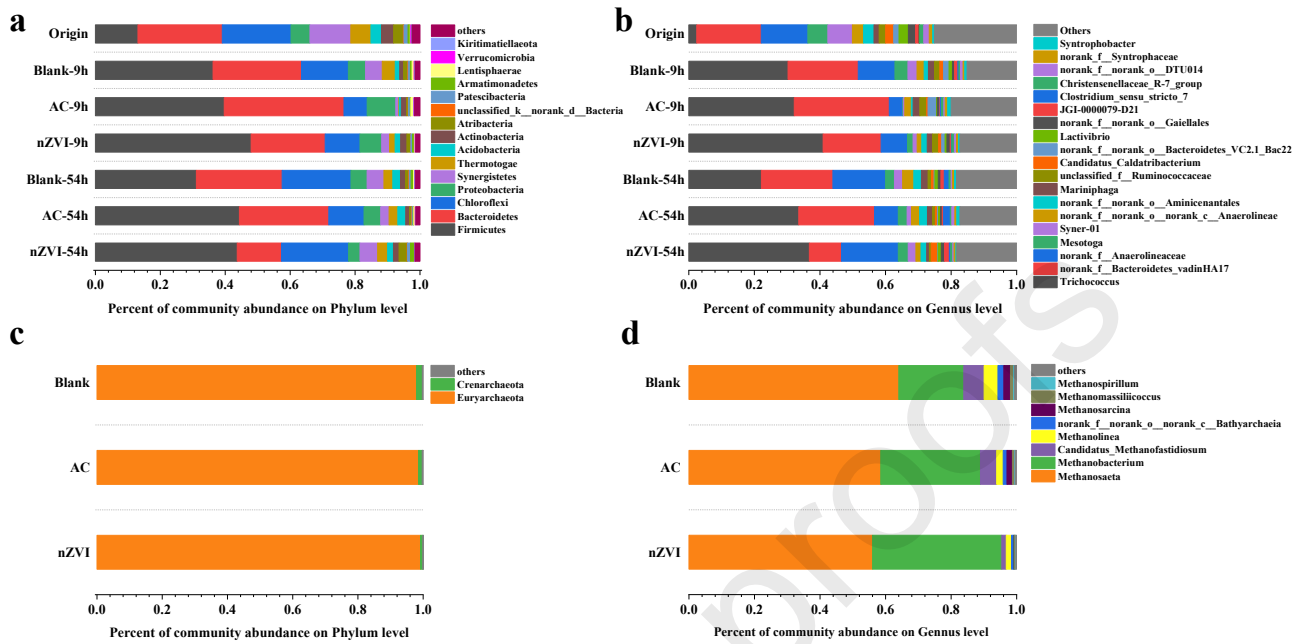
727

728

729

Fig. 2

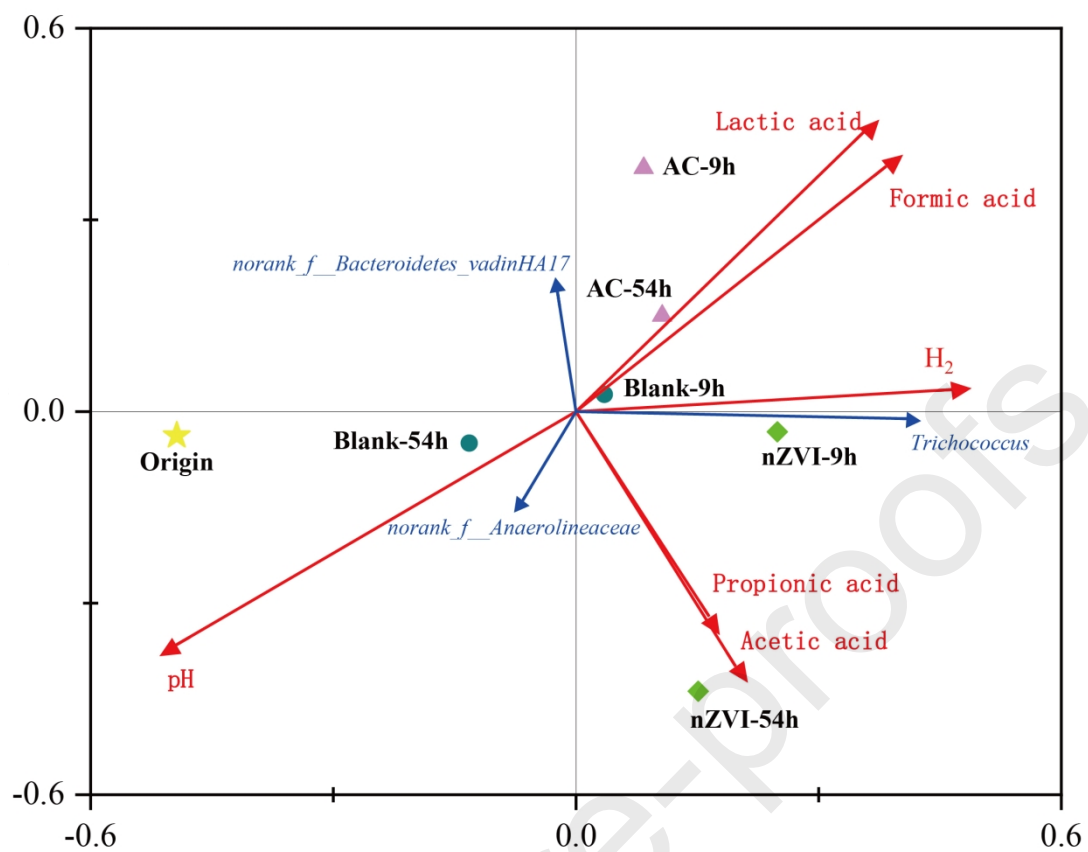
730



731

732

Fig. 3



733

734

Fig. 4

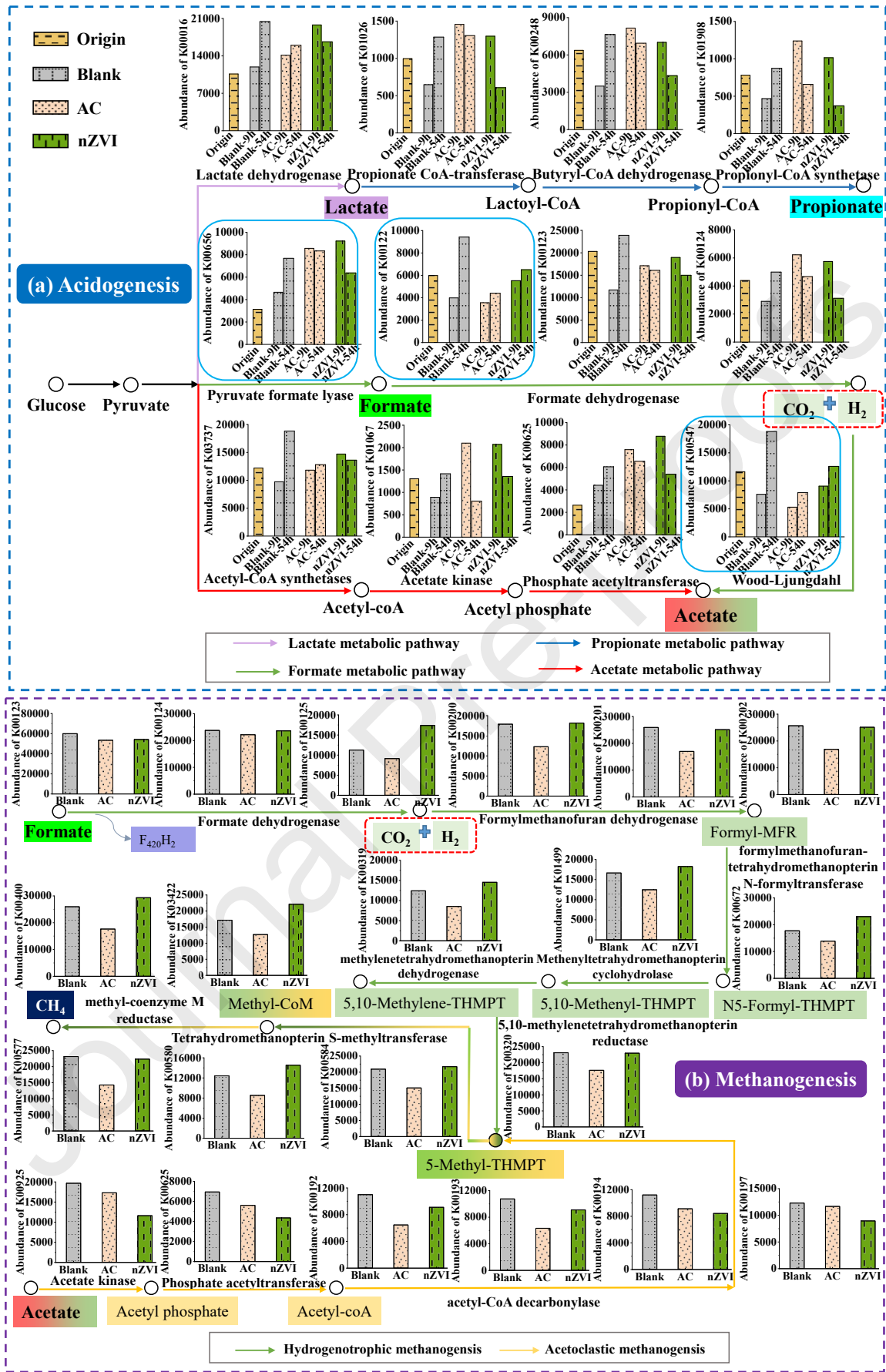


Fig. 5

736 53.

737 **Table 1** The performance of batch reactors under different conditions after the whole AD

Batch	pH	ORP (mV)	COD removal efficiencies (%)	Cumulative CH ₄ production (NmL)	CH ₄ yield (NmL CH ₄ /g COD)
Blank	6.88	-206.00	95.48%	23.88	250.11
AC	6.87	-197.00	96.89%	23.37	241.18
nZVI	8.48	-345.00	95.89%	29.72	309.89

738

739

740 54.

741 **Highlights**

- 742 1. Both AC and nZVI increased the production of VFAs in acidogenesis.
- 743 2. nZVI strengthened the formation of formic and acetic acids in acidogenesis.
- 744 3. nZVI is superior to AC on the enhancement of methane in whole AD.
- 745 4. *Methanobacterium* was selectively enriched with nZVI addition.
- 746 5. Mechanism of AC and nZVI on acidogenesis and whole AD was analyzed and
747 compared.

748

749 55.